Giant positive and negative Goos-Hänchen shift on dielectric gratings caused by guided mode resonance

Rui Yang, Wenkan Zhu, and Jingjing Li*

Department of Electrical and Computer Engineering, University of Illinois at Chicago, Chicago, IL, 60607, USA

**jili@uic.edu*

Abstract: Giant positive and negative Goos-Hänchen shift more than 5000 times of the operating wavelength is observed when a beam is totally reflected from a substrate decorated by a dielectric grating. Different to the former studies where Goos-Hänchen shift is related to metamaterials or plasmonic materials with ohmic loss, here the giant shift is realized with unity reflectance without the loss. This is extremely advantageous for sensor applications. The Goos-Hänchen shift exhibits a strong resonant feature at the frequency of guided mode resonance, and is associated to the energy flow carried by the guided mode.

OCIS codes: (130.0130) Integrated optics; (050.2770) Gratings; (260.5740) Resonance.

References and links

1. F. Goos and H. Hänchen, "Ein neuer und fundamentaler versuch zur totalreflexion," Annalen der Physik **436**, 333346 (1947).
2. M. Merano, A. Aiello, M. GWt Hooft, E. Eliel, and J. Woerdman, "Observation of goos-hanchen shifts in metallic reflection," Opt. Express **15**, 15928–15934 (2007).
3. X. Yin, L. Hesselink, Z. Liu, N. Fang, and X. Zhang, "Large positive and negative lateral optical beam displacements due to surface plasmon resonance," Appl. Phys. Lett. **85**, 372 (2004).
4. I. V. Shadrivov, A. A. Zharov, and Y. S. Kivshar, "Giant goos-hanchen effect at the reflection from left-handed metamaterials," Appl. Phys. Lett. **83**, 2713–2715 (2003).
5. R. W. Ziolkowski, "Pulsed and CW gaussian beam interactions with double negative metamaterial slabs," Opt. Express **11**, 662–681 (2003).
6. T. Hashimoto and T. Yoshino, "Optical heterodyne sensor using the goos-hänchennchen shift," Opt. Lett. **14**, 913–915 (1989).
7. X. Yin and L. Hesselink, "Goos-hänchen shift surface plasmon resonance sensor," Appl. Phys. Lett. **89**, 261108 (2006).
8. T.-K. Lee, G.-Y. Oh, H.-S. Kim, D. G. Kim, and Y.-W. Choi, "A high-q biochemical sensor using a total internal reflection mirror-based triangular resonator with an asymmetric MachZehnder interferometer," Opt. Commun. **285**, 1807–1813 (2012).
9. J. Sun, X. Wang, C. Yin, P. Xiao, H. Li, and Z. Cao, "Optical transduction of e. coli O157:H7 concentration by using the enhanced goos-hnchen shift," J. Appl. Phys. **112**, 083104 (2012).
10. X. Wang, C. Yin, J. Sun, H. Li, Y. Wang, M. Ran, and Z. Cao, "High-sensitivity temperature sensor using the ultrahigh order mode-enhanced goos-hänchen effect," Opt. Express **21**, 13380–13385 (2013).
11. Y. Wang, X. Jiang, Q. Li, Y. Wang, and Z. Cao, "High-resolution monitoring of wavelength shifts utilizing strong spatial dispersion of guided modes," Appl. Phys. Lett. **101**, 061106 (2012).
12. K. Artmann, "Annalen der physik 6," Band **2**, 87 (1948).
13. T. Tamir, "Nonspecular phenomena in beam fields reflected by multilayered media," J. Opt. Soc. Am. A **3**, 558–565 (1986).

#200072 - $15.00 USD Received 25 Oct 2013; revised 19 Dec 2013; accepted 9 Jan 2014; published 23 Jan 2014

14. K. Y. Bliokh and A. Aiello, “Goos-hächen and imbert-fedorov beam shifts: an overview,” J. Opt. **15**, 014001 (2013).
15. T. Tamir and E. Garmire, *Integrated optics* (Springer-Verlag, Berlin; New York, 1979).
16. R. H. Renard, “Total reflection: A new evaluation of the goos-hänchen shift,” J. Opt. Soc. Am. **54**, 1190–1196 (1964).
17. T. Tamir and H. L. Bertoni, “Lateral displacement of optical beams at multilayered and periodic structures,” J. Opt. Soc. Am. **61**, 1397–1413 (1971).
18. M. A. Breazeale and M. A. Torbett, “Backward displacement of waves reflected from an interface having superimposed periodicity,” Appl. Phys. Lett. **29**, 456 (1976).
19. A. Teklu, M. A. Breazeale, N. F. Declercq, R. D. Hasse, and M. S. McPherson, “Backward displacement of ultrasonic waves reflected from a periodically corrugated interface,” J. Appl. Phys. **97**, 084904 (2005).
20. S. W. Herbison, J. M. Vander Weide, and N. F. Declercq, “Observation of ultrasonic backward beam displacement in transmission through a solid having superimposed periodicity,” Appl. Phys. Lett. **97**, 041908 (2010).
21. M. Shokooh-Saremi and R. Magnusson, “Leaky-mode resonant reflectors with extreme bandwidths,” Opt. Lett. **35**, 1121–1123 (2010).
22. Y. Ding and R. Magnusson, “Band gaps and leaky-wave effects in resonant photonic-crystal waveguides,” Opt. Express **15**, 680–694 (2007).
23. C. J. Chang-Hasnain, “High-contrast gratings as a new platform for integrated optoelectronics,” Semicond. Sci. Technol. **26**, 014043 (2011).
24. M. C. Y. Huang, Y. Zhou, and C. J. Chang-Hasnain, “A nanoelectromechanical tunable laser,” Nat. Photonics **2**, 180–184 (2008).
25. C. Mateus, M. Huang, Y. Deng, A. Neureuther, and C. Chang-Hasnain, “Ultrabroadband mirror using low-index cladded subwavelength grating,” IEEE Photonic. Technol. Lett. **16**, 518–520 (2004).
26. S. S. Wang, R. Magnusson, J. S. Bagby, and M. G. Moharam, “Guided-mode resonances in planar dielectric-layer diffraction gratings,” J. Opt. Soc. Am. A **7**, 1470–1474 (1990).
27. R. Magnusson, “Flat-top resonant reflectors with sharply delimited angular spectra: an application of the rayleigh anomaly,” Opt. Lett. **38**, 989–991 (2013).
28. S. M. Norton, T. Erdogan, and G. M. Morris, “Coupled-mode theory of resonant-grating filters,” J. Opt. Soc. Am. A. **14**, 629–639 (1997).
29. D. Fattal, J. Li, Z. Peng, M. Fiorentino, and R. G. Beausoleil, “Flat dielectric grating reflectors with focusing abilities,” Nat. Photonics **4**, 466–470 (2010).
30. J. Li, D. Fattal, M. Fiorentino, and R. G. Beausoleil, “Strong optical confinement between nonperiodic flat dielectric gratings,” Phys. Rev. Lett. **106**, 193901 (2011).
31. L. Li, “New formulation of the fourier modal method for crossed surface relief gratings,” J. Opt. Soc. Am. A **14**, 2758–2767 (1997).
32. L. Li, “Formulation and comparison of two recursive matrix algorithms for modeling layered diffraction gratings,” J. Opt. Soc. Am. A **13**, 1024–1035 (1996).

1. Introduction

When a beam experiences a total internal reflection, a lateral shift exists between the reflected and the incident beams (see Fig. 1(a)). Named after its discoverers Goos and Hänchen [1], this effect is in striking inconsistency with the prediction of geometric optics. For decades, the phenomenon has been a research topic attracting considerable amount of efforts for its intriguing physical nature. It gained renewed attention in recent years when plasmonic materials and metamaterials are involved. Specifically, the negative GH shift on a plasmonic [2, 3] or metamaterial [4, 5] surface is among the mostly discussed problems. Sensor schemes based on GH shift has also been proposed [6, 7], and have led to sensors of biochemical [8, 9], thermal [10] and wavelength monitoring [11] applications. These engineering applications bring further interests beyond scientific curiosity to this phenomenon. The sensitivity in these sensors are directly related to the amount of GH shift, thus to achieve a large GH shift (positive or negative) is of practical interests. Designs of metamaterial waveguides that support a “frozen mode”, a waveguide mode that has no net energy propagation, are proposed by making use of the negative GH shift.

Mathematically, the shift is caused by the fact that different angular components of the incident beam experience different phase loss at the reflection. However, it took a long time for people to gain a deep understanding to the physical nature of the phenomenon [12–14]. The

#200072 - $15.00 USD Received 25 Oct 2013; revised 19 Dec 2013; accepted 9 Jan 2014; published 23 Jan 2014

GH shift had been generally understood as to account for the penetration of the evanescent field to the other side of the interface [15]. However, this interpretation faced difficulty in explaining the negative GH shift. In [16], the GH shift is related to the lateral energy flow carried by the evanescent wave beyond the interface of the total internal reflection. Whether the GH shift is positive or negative depends on the direction of this energy flow: when it is in the same direction of the projection of beam propagation direction on the interface, the shift is positive. Otherwise, negative GH shift happens. This explanation gives an intuitive understanding to the phenomenon, and can perfectly explain the negative GH shift on plasmonic and metamaterial interfaces. In a serial of theoretical works by Tamir [13, 17], the relationship between the GH shift and the leaky mode of multilayer and periodic structures are studied. Experimental works demonstrating his theory were carried out much more recently, but mostly on acoustic waves [18–20].

On the other hand, the leaky modes on dielectric gratings have found interesting applications in integrated optics [21–25]. In these studies, a Fano type resonance in the spectrum of the reflection coefficient is observed and used. Around the resonance, the magnitude of the reflection coefficient goes to 0 (total transmission), then 1 (total reflection), when the incident electromagnetic wave couples to the leaky mode. Because of the guided wave nature of the leaky mode, the resonance is commonly named guided mode resonance (GMR) under the context of dielectric gratings [22, 26]. This resonant feature has been used in broad band reflectors [25], sensors and filters [27, 28], planar lenses and cavities [29, 30], etc. In this paper, we study the possibility to use the GMR to achieve giant GH shift. Here, the leaky modes are excited in a way different to the former studies on GMR. The incidence comes from the substrate side of the grating at an angle greater than the critical angle of the substrate, and will be totally reflected from the surface of the substrate decorated by the dielectric grating (refer to Fig. 1(a)). When the incidence couples to the leaky mode of the grating, strong energy flow inside the waveguide exists, thus giant GH shift could be realized. When the leaky mode is a negative propagating one (i.e. the energy flow is anti-parallel to the wave vector of the mode), negative GH shift is expected.

2. Analysis

We consider a binary 1D grating of thickness t, period Λ and duty cycle Γ, defined as the ratio of the width of high index part (a) to the period, i.e. $\Gamma = a/\Lambda$ (refer to Fig. 1(a)). The two parts of the grating have relative permitivities of ε_h and ε_l ($\varepsilon_h > \varepsilon_l$), respectively. The grating sits on a substrate of relative permittivity ε_s. The permittivity of the cover is ε_c. We first study the dispersion property of the eigen modes propagating towards $+x$ direction, and the results for a silicon grating on a SiO_2 substrate ($\varepsilon_h = 12.12$, $\varepsilon_l = 1$, $\varepsilon_s = 2.09$, $\varepsilon_c = 1$) with duty cycle $\Gamma = 0.93$, thickness $t = 110$ *nm* and period $\Lambda = 430$ *nm* are shown in Fig. 1(b). Software package MEEP, a numerical electromagnetic solver based on the finite-difference time-domain algorithm is used to achieve the dispersion property. Both s (the only electric field component is parallel to the grating grooves) and p (the only magnetic field component is parallel to the grating grooves) polarized modes are studied. The dispersion curves show typical features of a periodic waveguide. For the s polarization, the lowest band is below the light line of the substrate, thus is confined to the grating structure and has no propagating components. In this band the mode is a conventional, positive mode (i.e. the power flow is at the same direction of the wave vector, here is $+\hat{x}$ direction). A gap shows up at the edge of the first Brillouin zone, above which lies the second band that is a negative propagating mode (energy flows towards $-\hat{x}$ direction). The lower part of this band is still below the light line of the substrate. As the operating frequency increases, the mode goes above the light line of the substrate when it begins to leak energy into the substrate, and finally above the free space light line when the

#200072 - $15.00 USD Received 25 Oct 2013; revised 19 Dec 2013; accepted 9 Jan 2014; published 23 Jan 2014

mode leaks to both sides. In the former studies of GMR for reflector and filter applications, it is usually the part above the free space light line that is used. Since GH shift is studied at total internal reflection, we are interested in the part between the two light lines when incidence is from the substrate side.

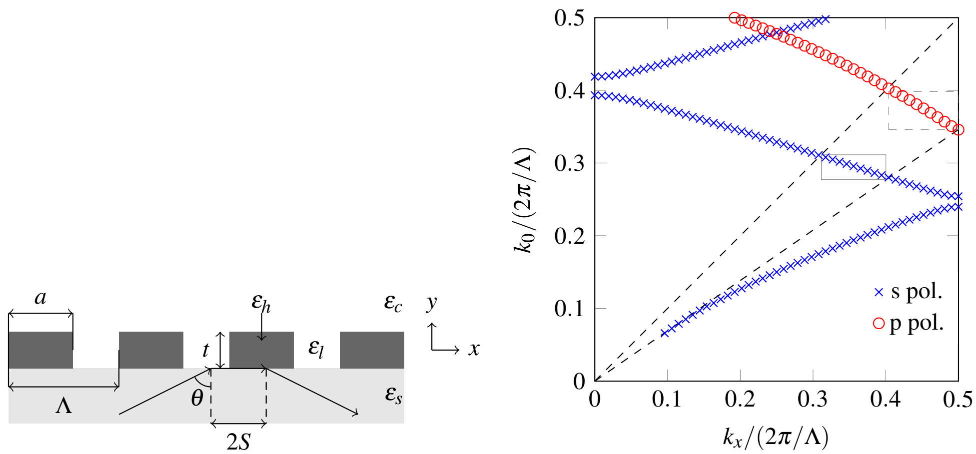

(a) (b)

Fig. 1. (a): Schematic of a dielectric grating and the GH shift under a total intenal reflection. Duty cycle is defined as $\Gamma = a/\Lambda$. (b): Dispersion curve for guided mode of s and p polarization for a grating of $\Lambda = 0.43\mu m$, $\Gamma = 0.93$, $t = 0.11\mu m$, $\varepsilon_h = 12.12$, $\varepsilon_l = \varepsilon_c = 1$ (free space), $\varepsilon_s = 2.09$ (SiO_2). The two dashed lines are the light lines of the free space ($k_0 = k_x$) and the substrate ($k_0 = k_x/\sqrt{\varepsilon_s}$), respectively.

Whereas the GH shift is defined for the incidence of a Gaussian beam, its numerical value at the limit of large beam size (compared to the wavelength) can be evaluated as [15]

$$S = -\frac{1}{k\cos\theta}\frac{\mathrm{d}\phi}{\mathrm{d}\theta} = -\frac{\mathrm{d}\phi}{\mathrm{d}k_x} \tag{1}$$

here θ is the angle of incidence of the Gaussian beam (i.e. the angle between the interface normal and the axis of the beam). k is the wavenumber inside the medium of the incident side, while $k_x = k\sin\theta$. ϕ is the phase of the reflection coefficient for a plane wave incidence at angle θ, at the same frequency. In Eq. (1) and throughout this paper, an $e^{-i\omega t}$ time variation of the fields is assumed. To study the GH shift, we first consider the reflection coefficient for a plane wave incidence from the substrate side with various incident angle (i.e. various k_x). The incidence is of s polarization with the electric field perpendicular to the plane of incidence. Through the paper, we select k_0 and k_x so that inside the substrate only the 0^{th} order diffraction (the direct reflection) is propagating, while all higher order diffraction modes are evanescent, while in the air both the 0^{th} and higher diffraction orders are evanescent. The free space wavelength of the incidence is $1.5\mu m$, corresponding to $k_0/(2\pi/\Lambda) = 0.287$. The phase of the reflection coefficient for k_x between the two light lines ($0.287 \sim 0.414 \times 2\pi/\Lambda$, or $43.8^\circ < \theta < 90^\circ$) is shown in Fig. 2(a) as a solid line. We notice that the magnitude of the coefficient remains 1 because of the total internal reflection. To get these results, a customized program based on rigorous coupled wave analysis (RCWA) [31, 32] is used. plot, we notice that the curve of the reflection coefficient phase exhibits sharp increases of almost 2π at around $k_x = 0.38 \times 2\pi/\Lambda$, or $\theta = 67.0^\circ$. From the dispersion results shown in Fig. 1(b), we notice that this k_x is exactly

#200072 - $15.00 USD Received 25 Oct 2013; revised 19 Dec 2013; accepted 9 Jan 2014; published 23 Jan 2014

the one when the guided mode at this frequency is excited. According to Eq. (1), the drastic increase of phase with k_x indicates a negative GH shift of giant magnitude. The curve of GH shift vs k_x is given in the same plot as a dashed line. As we can see, a sharp dip in the curve of GH shift is observed at the same k_x value when the phase exhibits a steep increases. At its maximum magnitude, the GH shift reaches a value of $-360\mu m$, about 240 times of the free space wavelength. The frequency dispersion of the GH shift for incidence at a fixed k_x is also studied and is shown in Fig. 2(b). Here $k_x = 0.38 \times 2\pi/\Lambda$ is used, a value corresponding to the one when GH shift achieves maximum magnitude in Fig. 2(a). As expected, the GH shift exhibits an obvious resonance peak, and the resonant frequency corresponds to that of the GMR. Such a resonant property has wide applications for sensors. We point out that, in our design, the giant negative GH shift is achieved when the magnitude of the reflection coefficient maintains unity. This is to the sharp contrast of some former studies when large negative GH shift is achieved at the cost of resonant ohmic loss with a reflectance towards 0 [7]. A large reflectance means better signal to noise ratio in sensor applications, thus is of great engineering importance.

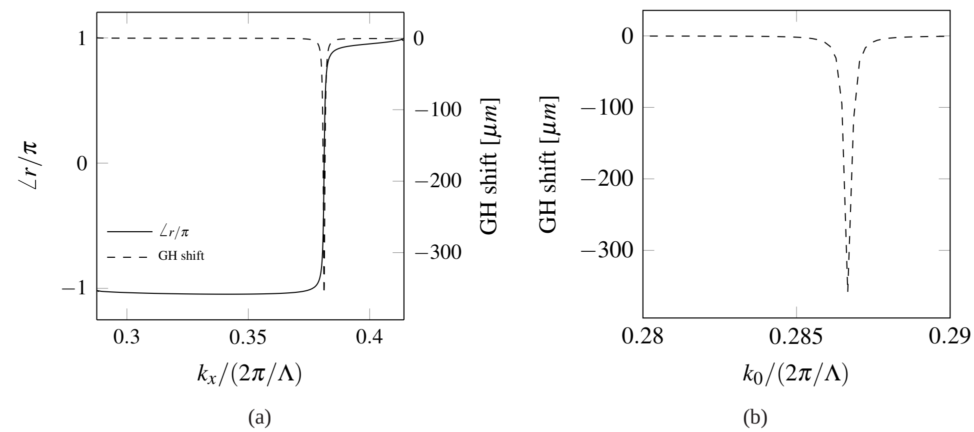

Fig. 2. (a): Phase of the reflection coefficient and GH shift vs k_x, for an incidence of $1.5\mu m$ free space wavelength from the substrate. (b): GH shift vs k_0 for an incidence from the substrate side with $k_x = 0.38 \times 2\pi/\Lambda$. The k_0 where the magnitude of the GH shift is maximized corresponds to the GMR frequency of the same k_x.

The field distribution inside and out of the grating at the resonance of GH shift is also checked to demonstrate explicitly the relationship between the resonant behavior of GH shift and the excitation of GMR. The results are shown in Fig. 3, where the color indicates the instantaneous distribution of E_z. The result in Fig. 3(a) is achieved at the condition ($1.5\mu m$ free space wavelength, $k_x = 0.38 \times 2\pi/\Lambda$) when GH shift is of the negative value of maximum magnitude. Notice that the incidence comes from the substrate ($y < 0$) from the lower left side. In the color plot, we notice that strong field around the grating is excited with a field strength much stronger than that of the incidence, which is identified as the guided mode of the grating. What is more interesting is the energy flow. The x component of the Poynting vector on a line parallel to $\hat{y}$ while going through the center of a grating period (refer to the white dashed line in the color plot of Fig. 3(a)) is plotted as a function of y and is placed next to the field plot. Notice that, around the grating ($0 < y < 0.11\ \mu m$), S_x shows an obvious dip of negative value. Far away from the grating inside the substrate, the field is a plane wave that is standing in y direction while propagating towards $+x$, thus a positive S_x is observed (see the inset of Fig. 3(b)). However, the maximum magnitude of negative S_x inside the grating is about 500 times larger than

#200072 - $15.00 USD Received 25 Oct 2013; revised 19 Dec 2013; accepted 9 Jan 2014; published 23 Jan 2014

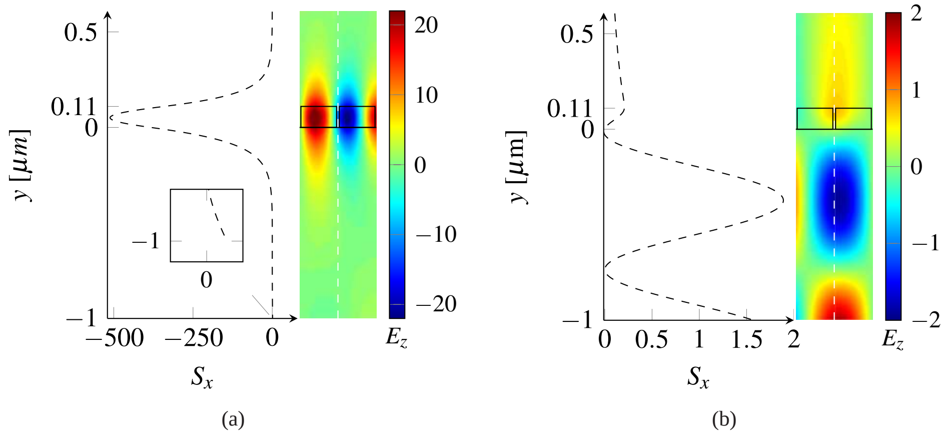

Fig. 3. Instantaneous distribution of electric field E_z (the color plot). The plot for the distribution of the x component of the Poynting vector (S_x) along the white dashed line is placed nearby. For the same system of Fig. 2 at 1.5 μm free space wavelength, with $k_x = 0.38 \times 2\pi/\Lambda$ (negative GH shift of maximum magnitude, (a)), or $k_x = 0.29 \times 2\pi/\Lambda$ (positive GH shift of 0.33 μm, 3b)

the positive S_x 1000 nm away from the grating. This is consistent with the explanation of GH shift in [16] where the negative GH shift is attributed to the negative energy flow beyond the reflection interface. For comparison purpose, we also give the results at a condition far from the GMR when a mediocre positive GH shift of 0.33μm is observed. This is shown in Fig. 3(b). As we can see, no obvious field enhancement inside the grating can be observed, and the energy still flows to the $+x$ direction inside the grating. The relationship between the GMR and the giant GH shift is most obviously seen in Fig. 4(a), where the GH shift for k_0 and k_x in the range inside the solid rectangle in Fig. 1(b) is shown. In this plot, the color is the GH shift, while the crosses are the eigenmodes on the dispersion curve inside the solid rectangle in Fig. 1(b). As we can see, the position of giant negative GH shift overlaps well with the guided mode of the grating.

The results shown above are for incidence of the s polarization. The p polarization shows similar results, as we see in Fig. 4(b). Again we study the part of the dispersion curve that is between the light lines of the free space and the substrate (dashed rectangle in Fig. 1(b)) where the incidence from the substrate can be totally reflected. Similar observation to that of the s polarization is made: GH shift exhibits a large negative value when the guided mode is excited. The maximum of the GH shift is, for this design case, even larger than that of the s polarization: a negative shift as large as 5700 μm is observed, more than 5000 times of the 1.08μm free space wavelength at the frequency.

A total reflection is usually required when discussing the GH shift. This limits the incidence to come from the substrate side at an angle larger than the critical angle, and it is the part of the dispersion curve between the light lines of the substrate and the free space that is used. Notice that the first band of the grating mode is a positive propagating mode and is below the light line of the substrate. Modes in this band can not be excited by an incidence from the substrate to achieve a positive GH shift, unless the whole structure is placed on a prism of higher refractive index, and frustrated total internal reflection is used to excite the modes. The next positive propagating band is the one above the second band gap (see Fig. 1(b)), and the part of this band in between the two light lines (not shown in Fig. 1(b)) can in principle be used to achieve giant

#200072 - $15.00 USD Received 25 Oct 2013; revised 19 Dec 2013; accepted 9 Jan 2014; published 23 Jan 2014

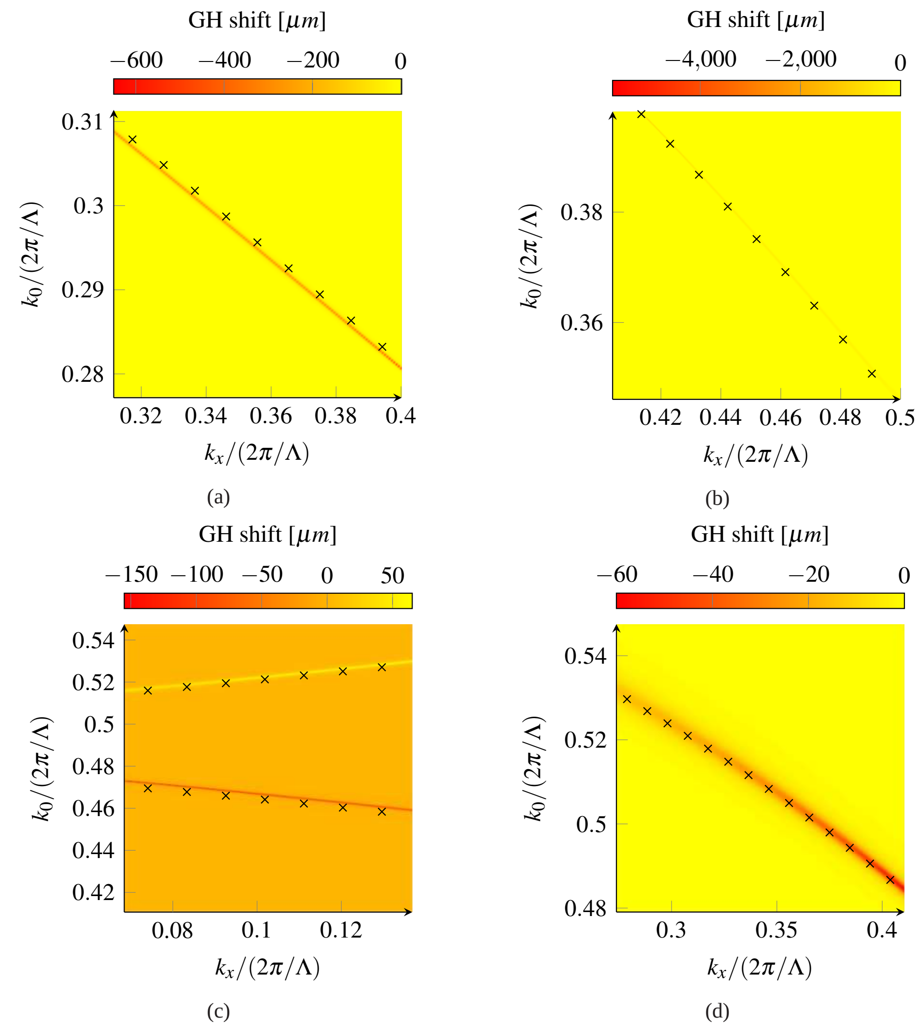

Fig. 4. Giant GH shift at different frequency and k_x. for s (a) and p (b) polarization of the grating studied in Fig. 2 corresponds to the framed areas. In (c), we give results for s polarization for the grating of the same design parameters of that studied in Fig. 2 but with a perfect electric conductor (PEC) substrate, while (d) is p polarization for the same grating design but half of the grating thickness. The crosses are the eigenmodes of the corresponding gratings.

#200072 - $15.00 USD Received 25 Oct 2013; revised 19 Dec 2013; accepted 9 Jan 2014; published 23 Jan 2014

positive GH shift. However, this usually happen at relatively high frequency, and care must be taken in designing the grating so that the first and higher order diffractions are still evanescent at this frequency.

When the incidence comes from the free space side, the grating considered in Fig. 2 and 3 gives a reflectance that in general is less than 1. To achieve unity reflectance for a broad incident angle, we can place the grating on top of a metal substrate. The metal surface is responsible for the total reflection while the dielectric grating can help provide a giant GH shift. The principle is similar, that is, giant GH shift exhibits when a guided mode is excited. Of course, the exact position of the GMR is different to that of Fig.1(b). Using an incidence from the air can be more convenient in many situations. Further more, since total reflection is promised for any k_x value, incidence close to the surface normal ($k_x \sim 0$) can be used (the case of Fig. 4(c)), so that the guided modes in the positive propagating band at relatively high frequency can be excited without worrying about bringing higher order diffraction modes into propagation. Positive GH shift can then be realized. We show the simulation results for a dielectric grating on a gold substrate in Fig. 4(c) (s polarization) and Fig. 4(d) (p polarization). For the sake of simplicity, here the metal is modeled as $\varepsilon = -\infty$ with no ohmic loss. The GH shift is shown as the color while the eigenmodes are marked as crosses. Besides the fact that giant negative GH shift is again observed at the GMR, several features deserve specific mentioning. First of all, giant negative GH shift can be observed for incidence of s polarization. This is to the direct contrary of the bare plasmonic substrate case where negative GH shift caused by surface plasmon only happens for the p polarization, while for s polarization, positive GH shift is observed. This is another proof that the grating decoration on top of the metal surface plays the crucial role in achieving the GH shift. Secondly, giant GH shift of positive value is indeed observed at the third eigenmode band, a positive propagating mode above the second band gap. This is shown in Fig. 4(c) (the first band, which is a positive mode band below the light line, is not shown in this plot).

3. Conclusion

In conclusion, we have used the GMR on dielectric gratings to realize giant GH shift. The giant GH shift is caused by the coupling of the incidence to the guided mode of the grating which are leaky on the incidence side. The large power flow carried by the guided mode is responsible for the giant GH shift. By exciting either a positive or a negative propagating mode, positive or negative GH shift is realized. Since the whole design is based on dielectric structure, ohmic loss can ideally be completely avoided and a unity reflectance can be realized. This is advantageous to many of the plasmonic material based approaches. We believe the design has great potential in sensor applications. Notice that a large GH shift happening in a finite reflection phase range ($\sim 2\pi$) usually means a sharp resonance with the incident angle (Fig. 2(a)), the frequency (Fig. 2(b)), the dielectric constant of the ambient environment (for example, the introducing of an agent), and other parameters. Such sharp resonances can be used for sensing with high sensitivity. The design also has wide application in slow light control, waveguide dispersion engineering, etc., which are currently under study.

Acknowledgments

Part of the work used the Extreme Science and Engineering Discovery Environment (XSEDE), which is supported by National Science Foundation grant number OCI-1053575. The Research Open Access Publishing (ROAAP) Fund of the University of Illinois at Chicago provides part of the publication fee for the open access of this article.

#200072 - $15.00 USD Received 25 Oct 2013; revised 19 Dec 2013; accepted 9 Jan 2014; published 23 Jan 2014